THE CURVE OF GROWTH OF GAMMA CYGNI

by

Frances Sherman Bailey

A Thesis

submitted to the faculty of the

Department of Physics

in partial fulfillment of

the requirements for the degree of

Master of Science

in the Graduate College

University of Arizona

1942

Approved: Franklin E. Roach, May 4, 1942

Director of Thesis Date

TABLE OF CONTENTS

CHAPTER		PAGE
I.	Introduction	1
II.	The Temperature of Gamma Cygni	17
III.	The Abundance of Fe I in Gamma Cygni	26
	Bibliography	30

Chapter I. Introduction

The curve of growth of a star is a plot showing the measured intensity of the absorption lines in the star's spectrum as a function of the number of absorbing atoms in the star's atmosphere. It will be shown that this plot may be used to determine the kinetic temperature of the star's atmosphere and other facts concerning the conditions at the surface of the star. In order to determine a curve of growth it is necessary to have a high-dispersion spectrogram of the star. The low-dispersion spectra which are used in most investigations of stellar spectra do not show enough unblended lines to make a curve of growth determination. As a result, curves of growth have been determined for only a few bright stars. Within the next few years astronomers hope to determine curves of growth for all of the brightest stars, including at least one of each spectral and luminosity class.

Gamma Cygni is a particularly interesting star because it has a temperature approximately equal to that of the sun whereas its luminosity is much greater. It is a supergiant star having a radius more than ten times that of the sun and a mean density equal to less than 1% of the mean density of the sun. Therefore a comparison between Gamma Cygni and the sun shows the difference between a large rarefied supergiant star and a relatively dense dwarf star of the same temperature.

The material used in the investigation consisted of two high dispersion spectra of Gamma Cygni taken with the Coudè spectrograph of the 82-inch reflector of the McDonald Observatory. The data for these two plates are

shown in Table I. Microphotometer tracings were made of these plates with the Moll microphotometer of the Steward Observatory. The tracings of Cd 139 were made by the author and those of Cd 38 were made by Mr. Jay E. Treat. The magnification of the scale of the plate on the tracing was determined by making a tracing of an accurate glass millimeter scale and was found to be 42.9 times.

Table I

Plate	Date	W. L. range	Linear dispersion Short W. L. end	Long W. L. end
Cd 139	1941, July 16	4000 to 4700	2.0 A/mm	5.4 A/mm
Cd 38	1940, Aug. 9	4400 to 6700	2.4 A/mm	16 A/mm

Both plates were provided with photometric standardization. Plate Cd 139 was accompanied by a spectrum made with the step spectrosensitometer of the McDonald Observatory. Standardization tracings were made across the step-spectrum at three places corresponding to wavelengths 4050, 4350, and 4650 approximately. Plate Cd 38 was standardized by means of two sets of spots made with the tube sensitometer of the McDonald Observatory. One set of spots was made with a red filter and the other with a green filter. Every measure of a spectral line was compared with the standardization traced on the same day whose wavelength was nearest that of the line.

The wavelengths and identifications of the lines in these spectra had already been measured by Dr. Roach[1]. From an inspection of this wave-

1. F. E. Roach, unpublished.

length table, two elements were selected for measurement of the curve of growth. The lines of the element Ti II were measured by the author and the lines of Fe I were measured by Mr. Jay E. Treat.

The reductions of the measures were made in the usual way. First a characteristic curve was drawn of density as a function of the logarithm of intensity for the standardization tracing. The density is as usual defined as the logarithm of the ratio of the clear plate scale reading to the reading on the standard step or spot. All readings were measured in millimeters from "total darkness", i.e., the position which is recorded on the tracing when no light enters the photocell of the microphotometer. The values of the intensities of the standardizations are known, and were supplied by Dr. Elvey of the McDonald Observatory. They are recorded in Table II.

Table II

Standardization Intensities

Step or Spot	Log Intensity of Step (Cd 139)	Log Intensity of Spot (Cd 38)
1	1.73	1.95
2	1.59	1.81
3	1.46	1.67
4	1.33	1.51
5	1.21	1.33
6	1.07	1.22
7	0.93	1.09
8	0.79	0.87
9	0.66	0.71
10	0.52	0.57
11	0.38	0.41
12	0.24	0.26
13	0.12	0.15
14	....	0.00

To get the total intensity of a spectral line, the tracing of the line is measured at intervals of 1 millimeter along the dispersion. The intensity corresponding to each measurement is obtained by entering

the density in the characteristic curve described above. The ratios of intensities in the line to the intensity of the continuous background are expressed in percent of intensity absorbed. Then a curve is plotted of per cent absorption as a function of distance along the dispersion. The area under this curve is a measure of the intensity of the line. The unit in which the area is expressed is the area of a rectangular absorption line which has an absorption of 100% and a width of 1 milli-Angstrom. The intensity of a spectral line expressed in these units is called the "equivalent width" in milli-Angstroms and is hereafter designated W. The areas were measured with a planimeter.

Most of the lines were measured with respect to the true continuous background of the spectrum. For a few of the lines, it was not possible to do this; and the lines were measured with respect to a local background whose intensity was below that of the true background because of the crowding together of blended spectral lines. For these lines, Thackeray's[2] ratio r is listed. The quantity r is the ratio of the intensity of the local background to that of the true background. As Thackeray has shown, the true equivalent width of a spectral line is to a first approximation the equivalent width measured with respect to the local background, divided by r.

In the case of lines which were blended on one side, the unblended side was measured and its equivalent width multiplied by two. For more seriously blended lines an estimation was made of the proportion of absorption due to the different members of the blend.

Five lines of Ti II which appeared on two tracings show that the probable error of a measurement of W is 13 milli-angstroms or about 4%.

---

2. Thackeray, Ap.J., 84, 433, 1936.

On the other hand, twenty lines of Ti II between $\lambda\lambda$4400 and 4700 which appeared on the overlap between Cd 139 and Cd 38 show a large systematic error between the two plates. The equivalent width measured on Cd 139 averages one-third higher than that on Cd 38.

This systematic error is almost certainly due either to a difference in reciprocity failure for the two plates or to the effect of comparing intensities integrated over a large wavelength range in the standard spots with monochromatic intensities in the spectrum. It is probably due to a combination of both of these causes.

In line spectrophotometry it is customary to ignore reciprocity failure. Spectra are taken at the telescope with long exposures of several minutes or hours depending on the brightness of the star and the type of emulsion and then are standardized by relatively short exposures of a few seconds or minutes in the sensitometer depending only on the type of emulsion. The characteristic curve obtained from the standardization is then assumed to be applicable to the spectrum, although students of photographic photometry know that it is in general not applicable. A difference in the error introduced by this false procedure in the case of the spectrosensitometer and tube sensitometer may explain our systematic error between the two plates.

Since this error is probably a function of wavelength and since the overlapping region for which it was determined is but a small portion of the entire spectral range, no attempt was made to reduce the measures of one plate to the scale of the other. For those lines which were measured on both plates, the average value of W was used. The systematic error produces a spurious probable error of about 35 milli-Angstroms.

Future investigators may avoid this error by determining the extent of reciprocity failure of the emulsion used and applying a corresponding correction to the characteristic curve of the standard.

Tables III and IV show the measured results for Fe I and Ti II, respectively. The excitation potentials and term designations were obtained from Miss Moore's A Multiplet Table of Astrophysical Interest. The final column in Tables III and IV will be discussed in Chapter II.

Dr. Roach's wavelength table for Gamma Cygni contains visual estimates of the strengths of the lines. Table V shows the average equivalent width for each visual intensity step up to 10, as determined by the Fe I and Ti II lines. Figure I shows the same material in graphical form.

Table III

Fe I Intensities (Treat)

W. L.	W (ma)	r	-Log W/λ	E. P. of Low Level	Multiplet	Log gf-χΘ
4071.72	427	1	3.98	1.601	$a^3F_2 - y^3F^o_2$	-1.59
4132.09	470	1	3.94	1.601	2 3	-2.13
4143.88	409	1	4.01	1.551	3 4	-1.97
4017.15	213	1	4.28	2.747	$a^3G_3 - w^3D^o_2$	
4011.43	63	1	4.80	2.548	$b^3F_4 - y^3G_5$	
4033.07	409	1	4.00	2.548	4 4	
4049.40	144	1	4.45	2.577	3 3	
4054.92	325	1	4.10	2.548	4 5	
4071.54	427	1	3.98	2.588	3 4	
4044.60	234	1	4.24	2.819	$b^3P_2 - z^3S^o_1$	-3.31
4062.43	298	1	4.14	2.853	1 1	-3.54
4079.85	206	1	4.30	2.846	0 1	-4.05
4091.57	55	1	4.87	2.819	$b^3P_2 - w^3D^o_1$	-4.61
4109.83	274	1	4.18	2.853	1 1	-2.64
4114.47	165	1	4.40	2.819	2 2	-2.63
4132.92	172	1	4.38	2.853	1 2	-3.11
4134.65	298	1	4.14	2.819	2 3	-3.38
4126.21	163	1	4.40	2.853	$z^5F^o - 18$	
4154.50	329	1	4.10	2.819	$b^3P_2 - y^3P^o_1$	-3.43
4184.91	208	1	4.30	2.819	2 2	-2.96
4191.49	411	1	4.01	2.846	0 1	-3.69
4202.03	541	1	3.89	2.853	1 2	-3.44
4147.67	338	1	4.09	1.478	$a^3F_4 - z^3G^o_3$	
4202.12	490	1	3.92	1.478	4 4	-2.11
4250.78	393	1	4.03	1.551	3 3	-2.18
4271.78	439	1	3.98	1.478	4 5	-1.67
4307.88	501	1	3.94	1.551	3 4	-1.60
4325.75	490	1	3.95	1.601	2 3	-1.59
4216.17	260	1	4.21	0.000	$a^5D_4 - z^7P^o_4$	-3.40
4239.81	300	1	4.15	2.681	$a^3G_5 - y^3G^o_5$	
4266.97	55	1	4.89	2.716	4 4	
4291.50	164	1	4.42	0.051	$a^5D_3 - z^7P^o_4$	-3.43

Table III (Cont'd)

W. L.	W (ma)	r	-Log W/λ	E. P. of Low Level	Multiplet	Log gf-χθ
4597.99	165	1	4.44	?	?	
4611.27	185	1	4.40	0.911	$a^5P_4 - z^5P_3^0$	
4618.79	320	1	4.16	2.936	$b^3G_5 - y^3G_4^0$	-5.19
4647.40	179	1	4.41	2.936	5 — 5	-3.82
4661.70	66	1	4.85	2.977	4 — 5	-5.24
4691.43	139	1	4.53	2.977	4 — 4	-3.97
4710.26	104	1	4.66	3.005	3 — 3	-4.08
4720.99	42	1	5.05	2.977	4 — 5	-5.23
4740.36	130	1	4.56	3.005	3 — 4	-5.26
4674.60	82	1	4.57	1.551	$a^3P_3 - z^3P_2^0$	
4924.84	235	1	4.32	2.269	$a^3P_2 - y^3D_2^0$	-4.12
5049.73	339	1	4.17	2.269	2 — 3	-3.37
5141.68	66	0.83	4.89	2.414	1 — 1	-4.27
5237.29	183	0.83	4.46	2.474	0 — 1	-4.19
4871.28	344	1	4.15	2.853	$z^7F_3^0 - e^7D_2$	
4872.12	314	1	4.19	2.870	1 — 1	
4878.18	327	1	4.17	2.873	0 — 1	
4890.72	380	1	4.11	2.863	2 — 2	
4891.54	308	1	4.20	2.839	4 — 3	
4903.29	285	1	4.24	2.870	1 — 2	
4919.03	309	1	4.20	2.853	3 — 3	
4920.53	616	1	3.90	2.820	5 — 4	
4957.48	673	1	3.87	2.839	4 — 4	
4985.36	346	1	4.16	2.853	3 — 4	
5044.15	184	1	4.44	2.839	4 — 5	
4939.69	218	1	4.36	0.855	$a^5P_5 - z^5P_4^0$	
4994.15	230	1	4.34	0.911	4 — 3	
5012.05	428	1	4.07	0.855	5 — 5	-3.46
5040.98	379	1	4.12	0.954	3 — 2	
5051.62	325	1	4.20	0.911	4 — 4	
5083.33	255	1	4.30	0.954	3 — 3	
5107.53	416	1	4.09	0.986	2 — 2	
5123.81	352	1	4.16	1.007	1 — 1	
5127.33	158	0.83	4.51	0.911	4 — 5	
5142.71	527	1	3.99	0.954	3 — 4	
5150.88	228	0.84	4.36	0.986	2 — 3	
5151.92	167	0.84	4.49	1.007	1 — 2	

Table III (Cont'd)

W. L.	W (ma)	r	-Log W/λ	E. P. of Low Level	Multiplet	Log gf-χθ
5041.76	505	1	4.00	1.478	$a^5P_4 - z^5P^0_3$	
5107.55	416	1	4.09	1.551	3 2	
5171.62	378	1	4.14	1.478	4 4	-3.06
5216.29	182	0.81	4.46	1.601	2 2	
5307.33	197	1	4.43	1.601	2 3	
5332.88	296	1	4.26	1.551	3 4	
5079.10	429	1	4.07	2.188	$a^5P_2 - y^5P^0_1$	
5098.67	318	1	4.20	2.167	3 2	
5198.73	104	0.89	4.70	2.213	1 2	
5202.32	347	1	4.18	2.167	3 3	
5250.72	335	1	4.20	2.188	2 3	
5167.36	561	1	3.95	1.478	$a^3P_4 - z^3D^0_3$	-2.64
5270.40	515	1	4.01	1.601	2 1	-2.91
5328.29	28	0.89	5.28	1.551	3 3	
5341.05	342	1	4.19	1.601	2 2	
5446.84	507	1	4.03	1.601	2 3	
5563.61	116	1	4.68	2.414	$a^3P_1 - y^3P^0_2$	
5328.29	28	0.89	5.28	0.911	$a^5P_4 - z^5D^0_3$	-2.47
5371.55	480	1	4.05	0.954	3 2	-2.69
5397.14	420	1	4.11	0.911	4 4	-2.94
5405.76	384	1	4.15	0.986	2 1	-2.86
5429.74	472	1	4.06	0.954	3 3	-2.88
5434.52	440	1	4.09	1.007	1 0	-3.11
5446.84	507	1	4.03	0.986	2 2	-2.99
5455.58	439	1	4.10	1.007	1 1	-3.10
5497.46	355	1	4.19	1.007	1 2	
5506.81	298	1	4.27	0.986	2 3	
5615.64	214	1	4.42	2.577	$b^3P_3 - y^3D^0_2$	
5667.16	348	1	4.21	2.597	2 2	
5701.52	99	1	4.76	2.548	4 3	
6065.53	224	1	4.43	2.597	$b^3P_2 - y^3P^0_2$	
6137.65	346	1	4.25	2.577	3 3	
6200.34	142	1	4.64	2.597	2 3	
6230.65	185	0.88	4.32	2.548	4 4	
6136.68	295	1	4.32	2.443	$a^3H_4 - z^3G^0_3$	-3.56
6191.46	282	1	4.34	2.422	5 4	-3.44
6252.62	180	1	4.54	2.394	6 5	-3.33
6256.20	156	1	4.60	2.443	4 4	-4.84

Table III (Cont'd)

W. L.	W (ma)	r	-Log W/λ	E. P. of Low Level	Multiplet	Log gf-χθ
6270.09	99	1	4.80	2.846	$b^3P_0 - y^3D^o_1$	
6355.16	158	1	4.60	2.853	$1 \quad 2$	
6254.21	246	1	4.41	2.269	$a^3P_2 - z^3P^o_1$	
6421.43	343	1	4.27	2.269	$2 \quad 2$	
6592.78	94	1	4.85	2.716	$a^3G_4 - y^3F^o_3$	

Table IV

Ti II Intensities

W. L.	W (ma)	r	-Log W/λ	E. P. of Low Level	Multiplet	$\text{Log}\frac{aSs}{\Sigma s} - \chi\theta$
4028.35	365	1	4.04	1.884	$b^2G_{4\frac{1}{2}} - y^2F^o_{3\frac{1}{2}}$	
5053.83	224	1	4.26	1.885	$3\frac{1}{2}$ $2\frac{1}{2}$	
4064.37	236	1	4.24	2.586	$b^2F_{2\frac{1}{2}} - y^2P^o_{1\frac{1}{2}}$	
4161.52	163	1	4.41	1.079	$a^2D_{2\frac{1}{2}} - z^4D^o_{3\frac{1}{2}}$	
4173.55	458	1	3.96	1.079	$2\frac{1}{2}$ $2\frac{1}{2}$	
4184.31	308	1	4.12	1.075	$1\frac{1}{2}$ $1\frac{1}{2}$	
4190.24	249	1	4.22	1.079	$2\frac{1}{2}$ $1\frac{1}{2}$	
4163.66	363	1	4.06	2.579	$b^2F_{3\frac{1}{2}} - x^2D^o_{2\frac{1}{2}}$	-0.53
4171.91	526	1	3.90	2.586	$2\frac{1}{2}$ $1\frac{1}{2}$	-0.70
4174.08	219	1	4.28	2.586	$2\frac{1}{2}$ $2\frac{1}{2}$	-1.84
4287.89	441	1	3.99	1.075	$a^2D_{1\frac{1}{2}} - z^2D^o_{2\frac{1}{2}}$	
4294.10	420	1	4.01	1.079	$2\frac{1}{2}$ $2\frac{1}{2}$	
4337.93	540	1	3.91	1.075	$1\frac{1}{2}$ $1\frac{1}{2}$	
4344.29	570	1	3.88	1.079	$2\frac{1}{2}$ $1\frac{1}{2}$	
4290.33	481	1	3.95	1.160	$a^4P_{1\frac{1}{2}} - z^4D^o_{2\frac{1}{2}}$	+0.29
4300.06	734	1	3.76	1.175	$2\frac{1}{2}$ $3\frac{1}{2}$	+0.55
4301.93	427	1	4.00	1.156	$\frac{1}{2}$ $1\frac{1}{2}$	-0.11
4307.91	533	1	3.90	1.160	$1\frac{1}{2}$ $1\frac{1}{2}$	0
4312.88	472	1	3.96	1.175	$2\frac{1}{2}$ $2\frac{1}{2}$	-0.10
4314.98	491	1	3.94	1.156	$\frac{1}{2}$ $\frac{1}{2}$	-0.10
4320.96	588	1	3.87	1.160	$1\frac{1}{2}$ $\frac{1}{2}$	-0.80
4330.71	345	1	4.10	1.175	$2\frac{1}{2}$ $1\frac{1}{2}$	-1.05
4316.80	319	1	4.14	2.039	$b^2P_{\frac{1}{2}} - z^2P^o_{1\frac{1}{2}}$	
4330.25	270	1	4.21	2.039	$\frac{1}{2}$ $1\frac{1}{2}$	
4350.84	377	1	4.06	2.052	$1\frac{1}{2}$ $1\frac{1}{2}$	
4341.37	323	1	4.13	1.11	$a^2G_{3\frac{1}{2}} - z^2D^o_{2\frac{1}{2}}$	
4367.68	399	1	4.04	2.579	$b^2F_{3\frac{1}{2}} - y^2G^o_{4\frac{1}{2}}$	-1.04
4386.86	303	1	4.16	2.586	$2\frac{1}{2}$ $3\frac{1}{2}$	-1.15
4374.82	576	1	3.88	2.052	$b^2P_{1\frac{1}{2}} - y^2D^o_{2\frac{1}{2}}$	
4421.95	290	1	4.19	2.052	$1\frac{1}{2}$ $1\frac{1}{2}$	

Table IV (cont'd)

W. L.	W (ma)	r	-Log W/λ	E. P. of Low Level	Multiplet	$\text{Log}\frac{aSs}{\Sigma s} - \chi\theta$
4391.04	283	1	4.19	1.226	$b^4P_{1\frac{1}{2}} - z^4D^o_{2\frac{1}{2}}$	
4395.85	325	1	4.13	1.238	$2\frac{1}{2}$ $3\frac{1}{2}$	
4411.94	304	1	4.16	1.219	$\frac{1}{2}$ $\frac{1}{2}$	
4423.27	145	1	4.49	1.226	$1\frac{1}{2}$ $\frac{1}{2}$	
4427.92	156	1	4.46	1.238	$2\frac{1}{2}$ $1\frac{1}{2}$	
4394.07	402	1	4.04	1.216	$a^2P_{\frac{1}{2}} - z^4D^o_{1\frac{1}{2}}$	
4399.78	522	1	3.92	1.232	$1\frac{1}{2}$ $2\frac{1}{2}$	
4407.65	383	1	4.06	1.216	$\frac{1}{2}$ $\frac{1}{2}$	
4418.34	369	1	4.08	1.232	$1\frac{1}{2}$ $1\frac{1}{2}$	
4432.09	177	1	4.40	1.232	$1\frac{1}{2}$ $\frac{1}{2}$	
4395.04	520	1	3.92	1.079	$a^2D_{2\frac{1}{2}} - z^2F^o_{3\frac{1}{2}}$	
4443.81	608	1	3.87	1.075	$1\frac{1}{2}$ $2\frac{1}{2}$	
4460.49	700	1	3.81	1.079	$2\frac{1}{2}$ $2\frac{1}{2}$	
4411.08	280	1	4.19	2.081	$c^2D_{1\frac{1}{2}} - x^2F^o_{2\frac{1}{2}}$	
4456.64	224	1	4.30	3.110	$2\frac{1}{2}$ $2\frac{1}{2}$	
4488.33	327	1	4.13	3.110	$2\frac{1}{2}$ $3\frac{1}{2}$	
4441.72	440	1	4.01	1.175	$a^4P_{2\frac{1}{2}} - z^2D^o_{2\frac{1}{2}}$	
4464.46	537	1	3.92	1.156	$\frac{1}{2}$ $1\frac{1}{2}$	
4470.86	630	1	3.85	1.160	$1\frac{1}{2}$ $1\frac{1}{2}$	
4495.43	140	1	4.50	1.175	$2\frac{1}{2}$ $1\frac{1}{2}$	
4444.56	410	1	4.04	1.111	$a^2G_{3\frac{1}{2}} - z^2F^o_{3\frac{1}{2}}$	-0.50
4468.50	545	1	3.91	1.126	$4\frac{1}{2}$ $3\frac{1}{2}$	+1.00
4501.28	526	1	3.93	1.111	$3\frac{1}{2}$ $2\frac{1}{2}$	+0.92
4469.16	419	1	4.03	1.079	$a^2D_{2\frac{1}{2}} - z^4F^o_{3\frac{1}{2}}$	
4493.53	214	1	4.32	1.075	$1\frac{1}{2}$ $2\frac{1}{2}$	
4506.74	212	1	4.32	1.126	$a^2G_{4\frac{1}{2}} - z^4F^o_{4\frac{1}{2}}$	
4545.14	368	1	4.09	1.126	$4\frac{1}{2}$ $3\frac{1}{2}$	
4524.69	557	1	3.91	1.226	$b^4P_{1\frac{1}{2}} - z^2D^o_{2\frac{1}{2}}$	
4544.02	276	1	4.22	1.238	$2\frac{1}{2}$ $2\frac{1}{2}$	
4568.33	258	1	4.25	1.219	$\frac{1}{2}$ $1\frac{1}{2}$	
4580.47	82	1	4.65	1.226	$1\frac{1}{2}$ $1\frac{1}{2}$	

Table IV (cont'd)

W. L.	W (ma)	r	-Log W/λ	E. P. of Low Level	Multiplet	Log $\frac{aSa}{\Sigma s} - \chi\theta$
4529.49	374	1	4.09	1.565	$a^2H_{4\frac{1}{2}}^{1} - z^2G^{o}_{4\frac{1}{2}}$	-0.90
4549.64	430	1	4.03	1.577	$5\frac{1}{2}$ $4\frac{1}{2}$	+0.81
4571.98	652	1	3.84	1.565	$4\frac{1}{2}$ $3\frac{1}{2}$	+0.73
4533.97	590	1	3.89	1.232	$a^2P_{1\frac{1}{2}}^{1} - z^2D^{o}_{2\frac{1}{2}}$	+0.29
4563.77	565	1	3.91	1.216	$\frac{1}{2}$ $1\frac{1}{2}$	+0.05
4589.96	544	1	3.92	1.232	$1\frac{1}{2}$ $1\frac{1}{2}$	-0.67
4549.62	430	1	4.03	1.175	$a^4P_{2\frac{1}{2}}^{1} - z^2P^{o}_{3\frac{1}{2}}$	
4609.27	182	1	4.54	1.175	$2\frac{1}{2}$ $2\frac{1}{2}$	
4629.34	474	1	3.99	1.175	$a^4P_{2\frac{1}{2}}^{1} - z^4P^{o}_{3\frac{1}{2}}$	
4636.33	152	1	4.49	1.160	$1\frac{1}{2}$ $2\frac{1}{2}$	
4655.71	228	1	4.31	1.156	$\frac{1}{2}$ $1\frac{1}{2}$	
4662.76	194	1	4.38	1.160	$1\frac{1}{2}$ $1\frac{1}{2}$	
4719.51	172	1	4.43	1.238	$b^4P_{2\frac{1}{2}}^{1} - z^2P^{o}_{2\frac{1}{2}}$	
4821.01	28	1	5.23	1.111	$a^2G_{3\frac{1}{2}}^{1} - z^4G^{o}_{3\frac{1}{2}}$	
4849.17	282	1	4.24	1.126	$4\frac{1}{2}$ $3\frac{1}{2}$	
4865.62	323	1	4.18	1.111	$3\frac{1}{2}$ $2\frac{1}{2}$	
4762.78	479	1	4.00	1.079	$a^2D_{2\frac{1}{2}}^{1} - z^4G^{o}_{3\frac{1}{2}}$	
4798.54	276	1	4.24	1.075	$1\frac{1}{2}$ $2\frac{1}{2}$	
4806.34	83	1	4.76	1.079	$2\frac{1}{2}$ $2\frac{1}{2}$	
4779.99	299	1	4.20	2.039	$b^2P_{1\frac{1}{2}}^{1} - z^2S^{o}_{\frac{1}{2}}$	
4805.10	397	1	4.08	2.052	$1\frac{1}{2}$ $\frac{1}{2}$	
4874.02	258	1	4.28	3.081	$a^2D_{1\frac{1}{2}}^{1} - y^2P^{o}_{1\frac{1}{2}}$	
4911.20	281	1	4.24	3.110	$2\frac{1}{2}$ $1\frac{1}{2}$	
5005.17	201	1	4.40	1.559	$b^2D_{1\frac{1}{2}}^{1} - z^4D^{o}_{1\frac{1}{2}}$	
5013.70	289	1	4.24	1.575	$2\frac{1}{2}$ $2\frac{1}{2}$	
5037.81	40	0.91	5.06	1.575	$2\frac{1}{2}$ $1\frac{1}{2}$	
5010.22	230	1	4.34	3.081	$c^2D_{1\frac{1}{2}}^{1} - x^2D^{o}_{1\frac{1}{2}}$	
5072.30	497	1	4.00	3.110	$2\frac{1}{2}$ $2\frac{1}{2}$	

Table IV (cont'd)

W. L.	W (ma)	r	-Log W/λ	E. P. of Low Level	Multiplet	Log $\frac{aS_s}{\Sigma s} - \chi\theta$
5129.16	423	1	4.08	1.884	$b^2G_{4\frac{1}{2}}^{1} - z^2G^{0}_{4\frac{1}{2}}{}_{1}$	
5131.31	142	0.83	4.48	1.885	$3\frac{1}{2}$ $4\frac{1}{2}$	
5183.74	755	1	3.83	1.884	$4\frac{1}{2}$ $3\frac{1}{2}$	
5185.91	421	1	4.09	1.885	$3\frac{1}{2}$ $3\frac{1}{2}$	
5154.08	572	1	3.95	1.559	$b^2D_{1\frac{1}{2}}^{1} - z^2D^{0}_{2\frac{1}{2}}{}_{1}$	-0.71
5188.70	519	1	4.00	1.575	$2\frac{1}{2}$ $2\frac{1}{2}$	+0.42
5226.55	930	1	3.75	1.559	$1\frac{1}{2}$ $1\frac{1}{2}$	+0.24
5262.15	519	1	4.00	1.575	$2\frac{1}{2}$ $1\frac{1}{2}$	-0.72
5211.54	173	0.89	4.43	2.579	$b^2F_{3\frac{1}{2}}^{1} - y^2F^{0}_{3\frac{1}{2}}{}_{1}$	-0.68
5268.62	291	1	4.26	2.586	$2\frac{1}{2}$ $2\frac{1}{2}$	-0.82
5336.80	432	1	4.09	1.575	$b^2D_{2\frac{1}{2}}^{1} - z^2F^{0}_{3\frac{1}{2}}{}_{1}$	+0.30
5381.03	356	1	4.18	1.559	$1\frac{1}{2}$ $2\frac{1}{2}$	+0.15
5418.78	321	1	4.22	1.575	$2\frac{1}{2}$ $2\frac{1}{2}$	-1.00
6491.59	888	0.98	3.85	2.052	$b^2P_{1\frac{1}{2}}^{1} - z^2D^{0}_{2\frac{1}{2}}{}_{1}$	

Table V

R. I.	Average W				
	Cd 139	Number of Lines	Cd 38	Number of Lines	Both Plates
1		0	101	11	101
2	63	1	93	5	88
3	144	1	202	14	198
4	131	5	259	19	232
5	245	5	322	24	309
6	301	16	337	22	322
7	352	5	440	10	408
8	490	8	501	14	467
9	486	3	658	1	529
10	438	15	440	2	438

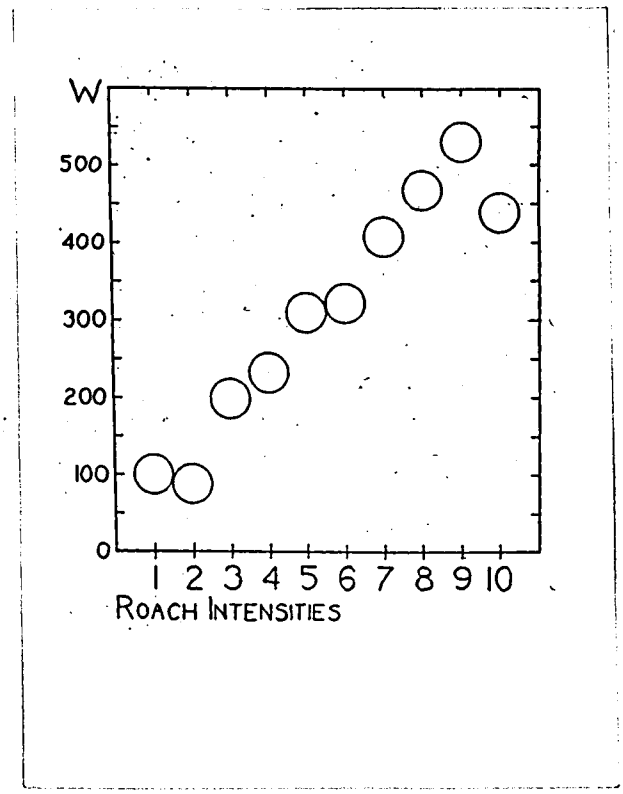

Figure 1. Equivalent width as a function of Roach's intensity estimates.

Chapter II. The Temperature of Gamma Cygni

In Chapter I the curve of growth was defined as the plot showing line intensity as a function of the number of atoms absorbing the line; and the method of measuring line intensity was explained. The methods of determining the number of atoms will now be discussed.

The number of atoms which absorb a line is equal to the number of atoms in the lower level of the line multiplied by the probability that an atom will make that transition. The number of atoms in the lower level is proportional to

$$ge^{-E/kT}$$

where g is the statistical weight $(2j+1)$ of the lower level, E is the excitation energy, k is the Boltzmann constant, and T is the temperature in degrees absolute. It will be convenient to deal with the common logarithm of the number of atoms and therefore the above expression is rewritten

$$g \cdot 10^{-\chi\theta}$$

where χ is the excitation potential of the lower level, and θ has the value 5040/T.

The relative probabilities of transitions obeying Russel-Saunders coupling have been computed. For a line this quantity may be designated as

$$\frac{aS_s}{\Sigma s}$$

The theoretical strength of the multiplet of which the line is a member is aS

and has been computed by Goldberg[3]. This quantity aS is the strength of a multiplet in terms of the quantity σ^2, a function of the total and orbital quantum numbers of the transition electron. Although the absolute value of σ is in general not known it is a constant for any given transition array which may include several multiplets. The relative intensity of the line in the multiplet is s, which has been tabulated by White and Eliason[4]. The relative intensity s divided by the sum of all the relative intensities Σs for the multiplet gives the fractional part of the multiplet strength contributed by the line. Since the multiplet strengths are relative, $\frac{aSs}{\Sigma s}$ gives only a relative value for the number of absorbing atoms. However, this could be given in absolute terms if the quantity α, mentioned above, were known.

In plotting a curve of growth the customary abscissa is log N f, where N is the number of atoms in the lower level per unit area of the star and f is called the "oscillator strength". It has the nature of a transition probability, but may be thought of as the atom's ability to absorb the line, expressed in terms of the absorptive power of a classical oscillator. For most atoms f is not known and it is therefore impossible to obtain the actual number of atoms. For a number of lines of Fe I, however, absolute values of f have been determined by King[5].

If two lines of Fe I have the same intensity, their values of N f must be equal. We know that N is proportional to $g \cdot 10^{-\chi\theta}$. Therefore if the

---

3. Goldberg, Ap.J., 82, 1, 1935, and 84, 11, 1936.
4. White and Eliason, Phys. Rev., 44, 753, 1933.
5. King, Ap.J., 87, 24, 1938, and 95, 78, 1942.

values of f, g, and χ for each line are known, the temperature may be computed. The temperature determined in this way is called the "excitation temperature".

An excitation temperature for Gamma Cygni was determined by this method using all the lines of Fe I for which the f values were available. For some lines not in King's table, the f values were determined from a plot made by Dr. Roach[1] which shows f as a function of $\frac{aS_s}{\Sigma^s}$ for Fe I lines in the sun.

To determine the excitation temperature log W/λ was plotted as a function of log gf for all lines. The lines arose from seven different lower levels. A curve was drawn through the points representing the lines arising from each level. The horizontal displacement of one of these seven curves with respect to another equals $(\chi_a - \chi_b)\theta$. Table VI shows the intersection of these seven curves with the horizontal line log W/λ = -4.4.

Table VI.

Determination of the excitation temperature of Gamma Cygni

Lower Level	χ	log gf (log W/λ = -4.4)
a^5D	0.026	-3.60
a^5F	0.953	-2.90
a^3F	1.55	-2.24
a^3P	2.41	-1.80
a^3H	2.42	-1.28
b^3P	2.83	-1.30
b^3G	2.97	-0.80

1. F. E. Roach, unpublished.

Figure II shows χ plotted as a function of

$$\log gf = \chi\theta + \text{constant}$$

The slope of the best straight line through these points is $1/\theta$. A least-squares solution yields

$$\theta = 0.909 \pm 0.005.$$

Therefore the excitation temperature is

$$T_{ex} = \frac{5040}{0.90} = 5600^{\circ} \text{ K}.$$

The curve of growth may now be plotted with abscissae equal to $\log gf - \chi\theta$. Let us first see what the nature of the curve will be. Minnaert and Mulders[6] were the first to explain the form of the curve of growth.

The atoms in the atmosphere of a star are not stationary but move with velocities which depend on the temperature according to the kinetic theory of gases. Therefore because of Doppler effect an absorption line formed by these atoms has a width proportional to the dispersion in velocity. As the number of absorbing atoms is increased the line will become deeper but not appreciably wider; and the increase in W/λ will be directly proportional to the number of absorbing atoms. As the central absorption approaches 100%, the curve of growth flattens out as $\log W/\lambda$ approaches a saturation value. Here another effect which tends to widen the lines becomes important. This effect is known as radiation damping. Radiation damping may be described in terms of the classical oscillator, which, as it absorbs light, vibrates with frequencies other than the fundamental. In this case the increase in W/λ is

---

6. Zeitschrift für Astrophysik, 1, 192, 1930, and 2, 165, 1931.

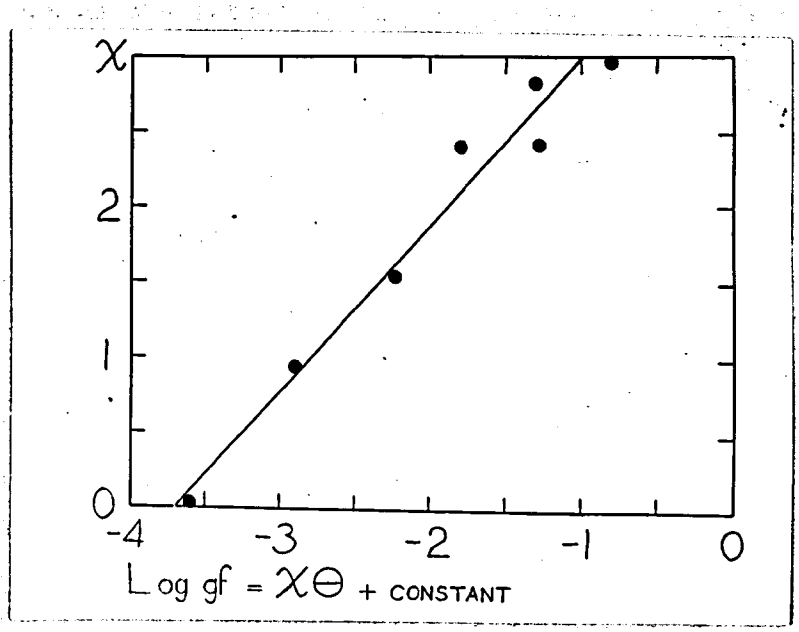

Figure II. The determination of $'\theta = 0.90$

proportional to the square root of the number of absorbing atoms. For a small number of atoms this effect is negligible compared with the thermal Doppler effect; but as the latter becomes saturated, the radiation damping continues to increase the intensity of the line.

A typical curve of growth therefore starts with a slope of 45° where W/λ is directly proportional to Nf. Then the slope decreases as W/λ approaches saturation. Finally the slope increases again to a maximum slope of 22°.5, where W/λ is proportional to $\sqrt{Nf}$. It is easy to see that for a star with a high temperature the 45° portion of the curve will be long whereas for a low temperature it will be short.

Figure III shows the curve of growth for Gamma Cygni. The two straight lines are the lines of thermal Doppler effect and radiation damping drawn from Miss Rubenstein's curve of growth for the sun[7] The curves of growth for Fe I (filled circles) and for Ti II (open circles) were adjusted horizontally until they were made to fit within the lines. The solid curve is the curve of growth for Gamma Cygni. For comparison, the dotted curve is that of the sun. Evidently Gamma Cygni has a higher temperature than the sun.

It is unfortunate that the lines of Fe I and Ti II for which relative intensities were available did not include lines very far from the flat portion of the curve of growth. The results can be strengthened if another element or other elements are measured which have lines on the two straight portions of the curve.

Five points on the curve were chosen for a determination of the velocity temperature. Menzel[8] has shown that the equation for the flat portion of the

---

7. P. J. Rubenstein, Ap. J., 92, 114, 1940.
8. Menzel, Ap. J., 84, 462, 1936.

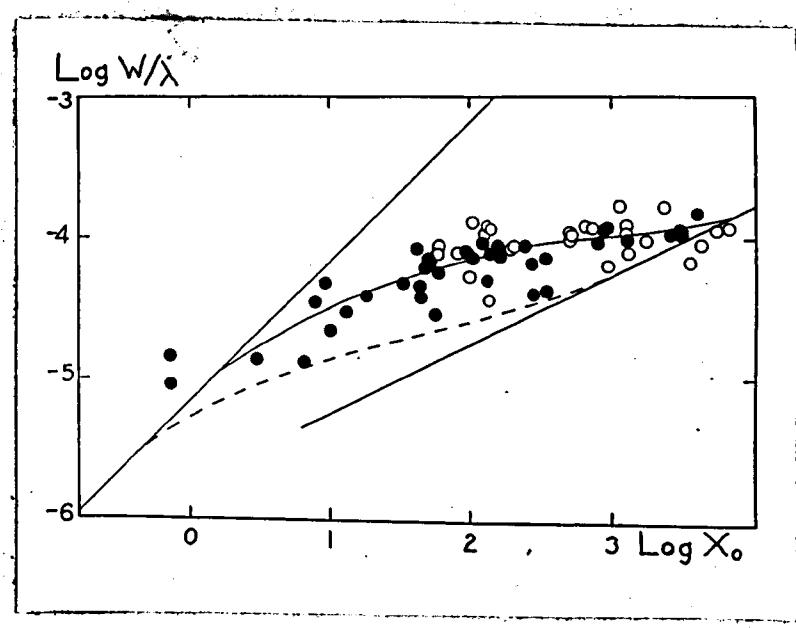

Figure III. The Curve of Growth of Gamma Cygni

curve of growth can be written:

$$\log \frac{W}{\lambda} = \log \left(X_o \frac{v}{c} \sqrt{\pi} \right) - \frac{1}{2} \log (1+X_o) - \frac{\frac{1}{2} \log \left(4\sqrt{\pi} \frac{v}{c} \frac{\nu^2}{\Gamma} \right)}{1 + 15\, e^{-2 \log X_o}}$$

where X_o = the central intensity of line (Harvard's abscissa for the curve of growth[7,8])

$\frac{v}{c}$ = thermal velocity in units of velocity of light

$\frac{\Gamma}{\nu} = 1.7 \times 10^{-6}$ (determined for the sun by Miss Rubenstein[7])

Table VII shows the five points that were used and the resulting values of v/c. Since Menzel's equation fits the middle portion of the curve best, only the three middle points were used in the determination of the most probable

Table VII

The velocity temperature of Gamma Cygni

Log W/λ	Log X_o	v/c	average of middle 3	v in km/sec	T_{vel}
-4.6	0.8	0.955×10^{-5}			
-4.4	1.2	1.513			
-4.2	1.8	2.24	2.30×10^{-5}	6.9	160,000°K
-4.1	2.2	3.16			
-4.0	2.8	1.78			

thermal velocity. This velocity was found to be 6.9 km/sec. This value is in good agreement with the velocity of 7 km/sec which Struve and Elvey[9] found for Alpha Persei, a star similar to Gamma Cygni in spectral type and

9. Struve and Elvey, Ap.J., 79, 409, 1934.

luminosity.

From the equation

$$v = \sqrt{\frac{2RT}{\mu}} \qquad \text{where } \mu = 55.8 \text{ (Fe)}$$

the velocity temperature can be computed. The value of T which results is 160,000°K.

Another method by which a star's temperature may be determined is the comparison of the spectral energy distribution of the star's radiation with a black-body distribution. The temperature so defined is called the "effective temperature". Kuiper[10] has made a table from which the effective temperature of a star is obtained as a function of spectral type and luminosity. Gamma Cygni is a giant F8 star; Kuiper's table gives an approximate value of 5600°K. The excitation temperature is also 5600°K.

The anomalously high value of the velocity temperature which occurs in some stars has been explained satisfactorily by Struve and Elvey as being due to turbulence. That is, there are macroscopic mass motions of the gas which makes up the star's atmosphere and this turbulent motion produces the effect of a temperature of 160,000°K. The actual temperature at the surface of Gamma Cygni is approximately 5600°K.

---

10. Kuiper, Ap.J., 88, 464, 1938.

Chapter III. The Abundance of Fe I in Gamma Cygni

The determination of absolute f-values for Fe I by King[5] makes it possible to determine the abundance of Fe I in stars for which the curve of growth is known. The number of atoms of an unionized element in a square centimeter column of the star's atmosphere is

$$N_o = \frac{\sum g \times 10^{-\chi\theta}}{g_i \times 10^{-\chi_i\theta}} \cdot N_i = BN_i$$

where N_i is the number of atoms in the level i. Or

$$\log N_o = \log B + \log N_i f - \log f.$$

The summation of $g \cdot 10^{-\chi\theta}$ is found to be 29.25. If log N f is known from the curve of growth, each line of Fe I yields a separate determination of N_o.

The line intensities were fitted to a curve of growth with abscissa log X_o[7,8]. The Harvard formula for X_o is

$$X_o = 1.152 \times 10^{-6} \lambda \sqrt{\frac{\mu}{T}} \; N f$$

Substituting the appropriate values:

λ = 5000 (an average value)

μ = 55.8 (Fe)

T = 160,000°K

then:

$$\log N f = \log X_o + 11.97.$$

Since the curve of growth yields log X_o as a function of log W/λ, N_o may be computed.

Table VIII shows the results of this computation for all unblended Fe I

lines for which f-values are available. The average value of N_o is

$$N_o = (4.4 \pm 2.6) \times 10^{18}$$

Roach and Phillips[11] and King[12] have determined N_o for the sun. The value by Roach and Phillips which was computed from the Harvard curve of growth is

$$N_o = (5.1 \pm 0.35) \times 10^{18}$$

These values indicate that the amount of unionized iron in a one square centimeter column of the atmosphere of Gamma Cygni is approximately the same as that of the sun. Since the temperature of Gamma Cygni is higher than that of the sun, and the pressure lower, the effects of both temperature and pressure must be to increase the number of ionized atoms of Gamma Cygni as compared with the sun. Therefore the total number of iron atoms may be higher in Gamma Cygni than in the sun.

It is a pleasure to thank Dr. F. E. Roach for the suggestion of the problem and for his guidance during its completion. I also wish to thank Dr. Otto Struve of the McDonald Observatory for the use of the plates and Dr. E. F. Carpenter of the Steward Observatory for the use of the Moll microphotometer. Special thanks are due to Mr. Jay E. Treat for his share in making the tracings and for his measurements of the Fe I lines.

---

11. Roach and Phillips, unpublished
12. King, Rp. J., 95, 82, 1942.

Table VIII

Abundance of Fe I in Gamma Cygni

Multiplet	λ	-Log W/λ	Log B	-Log f	Log N_o	$N_o \times 10^{-18}$
$a^3F - y^3F^o$	4071.72	3.98	2.21	0.85	18.17	1.48
	4132.09	3.94	2.21	1.38	18.87	7.41
	4143.88	4.01	2.01	1.43	18.25	1.78
$b^3P - z^3S^o$	4044.60	4.24	3.30	1.48	18.45	2.82
	4062.43	4.14	3.53	1.48	19.00	10.00
$b^3P - u^3D^o$	4091.57	4.87	3.30	2.70	18.32	2.09
	4109.83	4.18	3.53	0.58	17.98	0.95
	4114.47	4.40	3.30	0.80	17.30	0.20
	4132.92	4.38	3.53	1.05	17.83	0.68
	4134.65	4.14	3.30	1.55	18.84	6.91
$b^3P - y^3P^o$	4154.50	4.10	3.30	1.60	19.05	11.22
	4184.91	4.30	3.30	1.13	17.90	0.79
$a^3F - z^3G^o$	4202.12	3.92	1.84	1.73	18.93	8.51
	4250.78	4.05	2.01	1.62	18.25	1.78
	4271.78	3.98	1.84	1.30	18.12	1.32
	4307.88	3.94	2.01	1.06	18.30	1.99
	4325.75	3.95	2.21	0.85	18.21	1.62
$a^5D - z^7P^o$	4216.17	4.21	0.52	3.11	17.39	0.25
	4291.50	4.42	0.67	4.92	18.74	5.50
$b^3G - y^3G^o$	4647.40	4.41	3.07	2.22	18.47	2.95
	4661.70	4.85	3.20	2.51	19.07	11.74
	4691.43	4.53	3.20	2.24	18.34	2.19
	4710.26	4.66	3.32	2.23	18.20	1.58
	4720.99	5.05	3.20	3.50	18.80	6.30
$a^3P - y^3D^o$	4924.84	4.32	2.79	2.80	18.99	9.77
	5049.73	4.17	2.79	2.05	18.74	5.49
	5141.68	4.89	3.16	2.58	18.04	1.10
	5273.29	4.46	3.69	1.97	18.71	5.13
$a^5F - z^5F^o$	5012.05	4.07	1.20	3.73	19.22	16.59
$a^3F - z^3F^o$	5171.62	4.14	1.84	2.69	18.51	3.23

Table VIII (cont'd)

Multiplet	λ	-Log W/λ	Log B	-Log f	Log N_o	$N_o \times 10^{-18}$
$a^5F - z^5D^o$	5328.29	5.28	1.34	2.62	15.85	0.01
	5371.55	4.05	1.48	2.69	18.62	4.17
	5397.14	4.11	1.34	3.07	18.51	3.25
	5405.76	4.15	1.66	2.65	18.25	1.78
	5429.74	4.06	1.48	2.87	18.72	5.25
	5434.52	4.09	1.90	2.69	18.80	6.30
	4446.84	4.03	1.66	3.80	19.07	11.74
	5455.58	4.10	1.90	2.65	18.70	5.01
$a^3H - z^3G^o$	6136.68	4.32	2.72	2.31	18.45	2.82
	6191.46	4.34	2.61	2.30	18.27	1.86
	6252.62	4.54	2.51	2.29	17.67	0.47

BIBLIOGRAPHY

Goldberg, Leo — "Relative Multiplet Strengths in LS Coupling," Astrophysical Journal, 82, 1, 1935.

Goldberg, Leo — "Note on Absolute Multiplet Strengths," Ap.J., 84, 11, 1936.

Hertzberg, Gerhard — Atomic Spectra and Atomic Structure, Prentice-Hall, New York, 1937.

King, R. B. & King, A. S. — "Relative f-Values for Lines of Fe I and Ti I," Ap. J., 87, 24, 1938.

King, R. B. — "Absolute f-Values for Lines of Fe I," Ap. J., 96, 78, 1942.

King, R. B. — "Abundance of Iron in the Sun," Ap. J., 95, 82, 1942.

Kuiper, G. P. — "The Magnitude of the Sun, The Stellar Temperatus, Scale, and Bolometric Corrections," Ap. J., 88, 464, 1938.

Menzel, D. H. — "The Theoretical Interpretation of Equivalent Breadths of Absorption Lines," Ap. J., 84, 462, 1936.

Moore, Charlotte E. — A Multiplet Table of Astrophysical Interest, Princeton, N. J., 1933.

Rubenstein, Pearl J. — "The Kinetic Temperature of the Solar Reversing Layer," Ap. J., 92, 114, 1940.

Struve, Otto and Elvey, C. T. — "The Intensities of Stellar Absorption Lines," Ap. J., 79, 409, 1934.

Thackeray, A. D. — "Intensities of Blended Absorption Lines," Ap. J., 84, 433, 1936.

Unsöld, A. — Physik der Sternatmosphären, Berlin, 1938.

White, H. E. — Introduction to Atomic Spectra, McGraw-Hill, 1934.